Contrast Gain, Signal-to-Noise Ratio, and Linearity in Light-adapted Blowfly Photoreceptors

M. JUUSOLA, E. KOUVALAINEN, M. JÄRVILEHTO, and M. WECKSTRÖM

From the Department of Physiology, University of Oulu, Kajaanintie 52 A 90220 Oulu, Finland

ABSTRACT Response properties of short-type (R1-6) photoreceptors of the blowfly (*Calliphora vicina*) were investigated with intracellular recordings using repeated sequences of pseudorandomly modulated light contrast stimuli at adapting backgrounds covering 5 log intensity units. The resulting voltage responses were used to determine the effects of adaptational regulation on signal-to-noise ratios (SNR), signal induced noise, contrast gain, linearity and the dead time in phototransduction. In light adaptation the SNR of the photoreceptors improved more than 100-fold due to (*a*) increased photoreceptor voltage responses to a contrast stimulus and (*b*) reduction of voltage noise at high intensity backgrounds. In the frequency domain the SNR was attenuated in low frequencies with an increase in the middle and high frequency ranges. A pseudorandom contrast stimulus by itself did not produce any additional noise. The contrast gain of the photoreceptor frequency responses increased with mean illumination and the gain was best fitted with a model consisting of two second order and one double pole of first order. The coherence function (a normalized measure of linearity and SNR) of the frequency responses demonstrated that the photoreceptors responded linearly (from 1 to 150 Hz) to the contrast stimuli even under fairly dim conditions. The theoretically derived and the recorded phase functions were used to calculate phototransduction dead time, which decreased in light adaptation from ~5–2.5 ms. This analysis suggests that the ability of fly photoreceptors to maintain linear performance under dynamic stimulation conditions results from the high early gain followed by delayed compressive feed-back mechanisms.

INTRODUCTION

Photoreceptors respond to variable illumination, i.e., light contrasts, with changes of the membrane potential (reviewed by Shapley and Enroth-Cugell, 1984; Laughlin, 1989). This receptor potential is a result of the dynamic summation of elementary voltage responses, so-called quantum bumps, evoked by single photons (Yeandle, 1958; Fuortes and Yeandle, 1964; Wong, 1978). In dim light, single bumps can be distinguished, but as the amount of light is increased, bumps become smaller and

Address correspondence to Mikko Juusola, Department of Physiology, University of Oulu, Kajaanintie 52 A, 90220 Oulu, Finland.

J. GEN. PHYSIOL. © The Rockefeller University Press · 0022-1295/94/09/0593/29 $2.00
Volume 104 September 1994 593–621

faster and eventually fuse. This leads to strong adaptational desensitization whereby phototransduction maps the light changes superimposed on a 10^9-fold background range into a 50 mV response scale.

The coding of photoresponses has been proposed to be based on the light contrast, (c) between different objects (i.e., $c = \Delta I/I$), an invariance that does not change regardless of mean illumination (I) (Shapley and Enroth-Cugell, 1984). Previous studies of insect phototransduction have shown that long contrast steps elicit nonlinear responses (see Laughlin, 1989). This is mostly due to increasing compression (i.e., reduction of the amplitude) of photoresponses to light increments as the adapting background is increased, and differences between the molecular mechanisms behind excitation and deactivation (Laughlin and Hardie, 1978; Howard, Blakeslee, and Laughlin, 1987; Ranganathan, Harris, Stevens, and Zucker, 1991; Hardie and Minke, 1992; Juusola, 1993). Yet, Leutscher-Hazelhoff (1975), using delta-flashes, and experiments with white noise-modulated light stimuli by French (1980*b*,*c*) and by Weckström, Kouvalainen, and Järvilehto (1988) demonstrated that (with small modulation) light adapted fly photoreceptors operate approximately linearly. Recently, Juusola (1993) showed that in blowfly the stimulus-dependent linearity of the photoreceptor dynamics is related to the speed of the response integration. This suggests that the duration of the contrast stimulus, rather than its amplitude, accounts for the nonlinearity of photoresponses at any definite light adaptation state.

However, the number of photons absorbed by the photoreceptors depends not only on the intrinsic physiological and optical properties of the eye, but also on the motion of the animal relative to the contrast-rich edges in the environment and vice versa (Srinivasan and Bernard, 1975; Juusola, 1993). Therefore, in natural illumination, the contrasts to be detected by photoreceptors have a random, large amplitude and frequency variation. Such stimuli lead to a dynamically modulated phototransduction, where each effective photon elicits a bump whose latency and shape differs from other bumps coinciding to produce the actual sum-response. Because of this stochastic nature of the response summation, one could expect that the dynamic stimulus (as opposed to the static, i.e., background) may by itself cause additional noise to be added to the response and lead to deterioration of the photoreceptor's signal-to-noise ratio (Lillywhite and Laughlin, 1979). Hence, if one is to study the dynamics of photoreceptor contrast coding it is beneficial to use stimuli that cover a wide background range with sufficient frequency and amplitude variation of the contrast.

In this work we used a systems analysis approach to investigate adaptational regulation behind photoreceptor contrast coding. We considered a photoreceptor as an operational unit which receives certain input signal and generates, in a causal manner, a certain output signal. We investigated the response properties of short type (R1-6) photoreceptors of the blowfly (*Calliphora vicina*) with repeated sequences of pseudorandomly modulated light contrasts. This stochastic stimulus, simulating the contrast changes detected by a fast moving fly, allowed us to analyze the factors that cause noise and contribute to the photoreceptor's coding efficiency. With these methods, we were able to verify that the contrast stimulus itself does not alter the noisiness of the responses, and regardless of its amplitude did not generate

nonlinearities. We also determined the photoreceptor SNR and contrast gain in the frequency domain. The analysis also yields an estimation of so-called dead time or pure time delay in phototransduction over a background range of 10^5 log intensity units. Based on these results we argue that the adaptational compressive nonlinearities, along with strong negative feedback, act with a definite delay. This is responsible for the unexpectedly high linearity of the responses of light adapted photoreceptors.

METHODS

Animals and Preparation

We used wild-type adult blowflies (*Calliphora vicina*). The flies were cultured in the laboratory and fed on sugar and yeast and the larvae on liver. The stock was frequently refreshed with wild flies. For recording, the flies were attached to a small recording platform with beeswax. The Ag/AgCl indifferent electrode was located inside the head capsule near the retina being used. Sufficient ventilation was assured by leaving the abdomen mobile and not blocking the spiracles. The glass capillary microelectrodes were introduced by a piezoelectric microtranslator (Burleigh inchworm PZ-550) into the retina through a small hole made laterally on the left eye. The surface of the hole was sealed with high vacuum silicon grease. Intracellular recordings were performed from R1-6 photoreceptor somata (Weckström, Juusola, and Laughlin, 1992) at room temperature (20 ± 2°C) and began after 30 min of dark adaptation. The typical negative-onset ERG and continuous microelectrode penetrations of photoreceptors only were used to obtain the correct (retinal) recording location. R1-6 photoreceptors were identified by an input resistance of ~30 MΩ and by characteristic response properties—form, latency and duration—(e.g., Järvilehto and Zettler, 1971; Hardie, 1979; Weckström, Hardie, and Laughlin, 1991), which were tested in the dark before and after the recording procedures (see Fig. 2). The resistances of the microelectrodes, filled with 3 M KCl, were between 80 and 200 MΩ.

Light Stimuli

The light source was a green light emitting diode (LED) (Stanley HBG5666X, 510–600 nm, with peak emission at 555 nm) driven by a computer-controlled current source. The light output/current relation of the LED was limited to its linear range, which was tested during light stimulation using a pin diode circuit. The LED was fixed in a cardan arm system, which allowed free movement of the light source at a constant distance (50 mm) from the eye of the fly mounted at the center of rotation of the system. The light intensity level of the adapting background and sequences of pseudorandomly modulated contrast stimulus were generated and recorded with a microcomputer (IBM 486 compatible) using an ASYST (Keithley MetraByte, Taunton, MA) based program. The sequences of band-limited, pseudorandomly modulated stimulus had a Gaussian amplitude distribution and were spectrally white up to ~150 Hz (Fig. 1 *B* and *C*). Contrast (c) was defined as the standard deviation of the light stimulus sequence (σ_I) divided by the mean intensity (μ_I) of the adapting background (Fig. 1 *A*):

$$c = \frac{\sigma_I}{\mu_I} \tag{1}$$

Stimulating the photoreceptors with pseudorandomly modulated light has some advantages over the more conventional impulse stimulus or step approach. Only by this kind of stimulation it is possible to accurately control a photoreceptor's adaptational state and, at the same time, mimic light signals encountered naturally by the photoreceptors (Laughlin, 1981). The estimation of the frequency responses enabled us to evaluate the linearity of the system with the

help of the coherence function (French, Holden, and Stein, 1972; Marmarelis and Marmarelis, 1978). Also, long lasting adaptational processes could be characterised, subject to limitations imposed by the stimulus duration.

Different light contrasts, averaging from 0.04 to 0.42, were used in both signal-to-noise estimations and frequency response recordings. Although the contrasts used were rather small on average, it should be noted that they contained, by their Gaussian nature, intensity changes

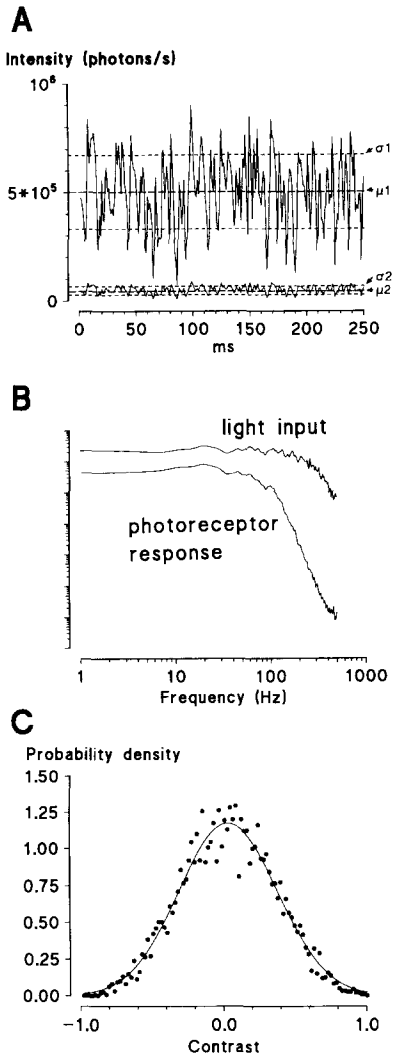

FIGURE 1. Properties of pseudorandomly modulated light contrast stimulus. (*A*) 250-ms samples of the stimulus sequence with contrast of 0.32 at two different mean intensity levels, i.e., adapting backgrounds. The contrast of the stimulus is defined as explained in the text. (*B*) The power spectra of the pseudorandom light input and of 210-times averaged photoreceptor responses at the adapting background of $5.0 \cdot 10^5$ photons/s. Note how the input spectrum is approximately flat up to 200 Hz, well beyond the 3 dB cut-off frequency of the output power spectrum (of the photoreceptor response). Signals were filtered at 500 Hz. (*C*) The probability density function of the amplitude of the pseudorandom stimulus shows the Gaussian distribution of the stimulation intensity.

that transiently decreased to complete darkness or more than double the mean intensity. For contrast higher than 0.32 (that was used for most of the experiments), the amplitude distribution of the stimulus had to be programmed to favor light increments in order to reach the desired high (mean) contrast values. This was because negative contrasts cannot be larger than -1 (the light decrement reaches zero intensity, i.e., darkness).

The light output of the LED was calibrated by counting, after prolonged dark adaptation, the number of discrete responses (evoked by single photons; Lillywhite, 1977) occurring during prolonged dim illumination. The unit of intensity, 1 effective photon s^{-1}, was defined to be that which elicited, on average, one quantal event per second in the dark-adapted photoreceptor. All the intensity values are expressed on the basis of this calibration as photons/s. The available intensity range was attenuated by neutral density filters (Eastman Kodak Co., Rochester, NY) to give a transient range of more than 6 log intensity units and a background illumination range of more than 5 log units. The lowest adapting background applied was ~200 effective photons/s. The light source subtended about two degrees at the photoreceptor level.

Recording Procedures

Flies were allowed to adapt for 90 s to the adapting background before introducing a prefixed number of pseudorandomly modulated sequences of light contrast. This was to ensure that the sensitivity of the photoreceptors had reached a steady state (Suss-Toby, Selinger, and Minke, 1990) and that most forms of adaptation, including any pupil response were completed (see Howard et al., 1987). The photoreceptor voltage response to the stimulus sequence was recorded intracellularly. The microelectrode was connected to a high impedance preamplifier (SEC-1L, NPI Electronics, Tamm, Germany), low-pass filtered at 500 Hz (KEMO VBF/23 elliptic filter), and sampled at 2 kHz along with the monitor voltage of the LED intensity. Both the voltages were then digitized with a 12-bit A/D converter (DT-2821, Data Translation, Marlboro, MA) and stored on hard disk. The frequency response of the recording system, including the microelectrode, had a 3 dB high frequency cut off at 10 kHz or higher, and did not affect the results.

The sampling process was initiated synchronously to the cycle of the pseudorandom noise signal generated by the computer. The 8-s records of both voltages obtained during each cycle were converted to suitable units (photoresponses to mV; LED current records to contrast units or photons/s). A 6-s stimulus interval of mean steady background was maintained between every consecutive contrast sequence to ensure that light adaptation was equal for each repeated stimulus sequence. After a preset number of stimulation runs, the average response was calculated. The averaged data were then segmented for FFT analysis using a Blackman-Harris four-term window with 50% overlap of the segments (Harris, 1978). Auto- and cross-correlation spectrum estimates were calculated with a FFT algorithm. After frequency-domain averaging of the spectra of different segments, the frequency response, coherence function and the first order Wiener kernels were calculated (French et al., 1972; French and Butz, 1973; Marmarelis and Marmarelis, 1978). To maintain a steady increase in light adaptation, the recordings were first performed at the lowest adapting background before proceeding to higher adapting backgrounds. For contrast experiments with fixed background, the stimulus contrast was increased from the smallest to the largest contrast value. After light adaptation the cells were re-dark adapted. A recording was rejected if the sensitivity and time courses of step responses did not return to their initial values.

Signal-to-Noise Analysis in the Time and Frequency Domains

The signal-to-noise ratio (SNR) between the photoresponse (signal) produced by the pseudo-randomly modulated stimulus and the voltage (noise) induced by the light background was calculated at different adapting backgrounds in both the time and frequency domain (for details, see Kouvalainen, Weckström, and Juusola, 1994). The signal-to-noise analysis in time domain was performed in the following way: after the initial dark adaptation period the variance of the photoreceptor voltage fluctuation (noise) was calculated from 10 to 30 2-s samples at each adapting background, yielding the variance of the background induced noise

(σ^2_{bn}). The variance of the total noise (σ^2_{cr}) was obtained during pseudorandom stimulation, superimposed on the background, so that the mean intensity remained the same as with the background alone. The variance of the photoreceptor signal (σ^2_{ps}) was calculated by subtracting the variance of background induced noise from the variance of the contrast-induced response recorded at the same adapting background.

$$\sigma^2_{ps} = \sigma^2_{cr} - \sigma^2_{bn} \tag{2}$$

The photoreceptor SNR was then obtained from the ratio

$$SNR_{phr} = \frac{\sigma^2_{ps}}{\sigma^2_{bn}} \tag{3}$$

The same procedure was repeated for each background intensity.

The calculation of the SNR in the frequency domain was based on time domain averaging of the photoresponses elicited by the pseudorandom contrast stimulus (French, 1980*a*), made possible by the repeated presentation of the same pseudorandom sequence. The time domain averaged photoreceptor signal was used in two ways: for the calculation of the signal power spectrum and for determining the signal-induced noise. The latter was achieved by subtracting the averaged response from the individual nonaveraged responses. SNR in frequency domain was finally calculated by dividing the signal power spectrum by the power spectrum of the total noise.

Calculation of the Effective Duration of the Quantum Bumps

The noise spectra obtained by subtracting dark noise from the background-induced noise was used to calculate the effective duration of the discrete voltage event caused by absorption of a single light quantum, i.e., a so-called bump. The procedure has been described in detail earlier (Dodge, Knight, and Toyota, 1968; Roebroek, van Tjonger, and Stavenga, 1990; Suss-Toby et al., 1991). Shortly, assuming a bump shape given by the Γ-distribution:

$$\Gamma(t;n,\tau) = \frac{1}{n!\tau}\left(\frac{t}{\tau}\right)^n e^{-t/\tau} \tag{4}$$

the two parameters, n and τ, can be obtained by fitting the following to the experimental power spectra of the noise:

$$[\Gamma(f;n,\tau)]^2 = \frac{1}{(1 + (2\pi\tau f)^2)^{n+1}} \tag{5}$$

where f is the frequency. The effective duration of the bump (i.e., the duration of a square pulse with equivalent power) is then calculated as:

$$T = \tau \frac{(n!)^2 2^{2n+1}}{(2n)!} \tag{6}$$

Photoreceptor Frequency Response and Dead Time

The photoreceptor frequency response function was calculated from the contrast stimulus and photoreceptor response, as two real-valued functions of frequency. (*a*) Gain, $G(f)$, the ratio of the photoreceptor response amplitude (mV) to the contrast stimulus amplitude (contrast units). (*b*) Phase, $P(f)$, the phase shift between the stimulus and the response. The coherence function calculated along with the frequency response function gives an index of nonlinearities and the signal-to-noise ratio of the system (Bendat and Piersol, 1971). From the transfer functions thus

obtained it is also possible to calculate the linear impulse response of the system, or the first order Wiener kernel (h_1), via the inverse Fourier transform (French et al., 1972; French and Butz, 1973; Marmarelis and Marmarelis, 1978).

When the analytical form of the gain function is known, a corresponding phase function can be calculated. Any deviations from this phase shift can be attributed either to a pure time delay (dead time) element or to some more exotic system property, like an all-pass type lattice network (Johnson, 1976). The latter possibility is unlikely, because those type of systems require inductance-like elements, which is difficult to reconcile with the present ideas of phototransduction. Therefore, by comparing the calculated phase function to the experimentally determined phase we can safely assume that we obtained the dead-time of the system. For details of this procedure see Appendix.

RESULTS

The following a priori criteria were used to ensure that only cells which showing excellent recording stability were chosen for further experiments: (*a*) In recordings from the dark adapted R1-6 photoreceptors, the resting potentials of the cells were −60 mV or below, (*b*) the saturating values of receptor potentials were over +55 mV, and (*c*) the input resistances were at least 30 MΩ (Weckström et al., 1991). Altogether, 88 cells which fulfilled these criteria were used in the analysis reported here. All findings were confirmed in at least six experiments, unless otherwise stated. The response characteristics described below were seen in every recording under similar conditions.

Fig. 2 *A* illustrates the characteristic voltage responses of a R1-6 photoreceptor to a series of 300-ms light pulses of exponentially increasing intensity. Although saturating voltage responses (to bright steps in the dark adapted state) are only rarely induced by natural contrasts, this test provided—along with the input resistance—a good measure of the cell's physiological condition and a fairly good prognosis of the stability of the cell impalement. Additionally, after 90 s of light adaptation to a steady light background, the photoreceptors were tested with a series of 300 ms contrast pulses (Fig. 2 *B*). This procedure was also useful for monitoring the condition of the photoreceptor.

The responses elicited by both test stimuli demonstrated one of the well known but fundamental properties of adaptational regulation in photoreceptors, namely that the nonlinearities produced by long lasting stimuli are mainly compressive. In Fig. 2 *B* the step responses (for contrasts >0.2) are nonlinear with respect to positive contrasts and asymmetric vis a vis polarity. Dark or light adapted, blowfly photoreceptors respond to light pulses by a rapid change of their membrane potential, depending on the stimulus intensity. If the light stimulus is sustained, the photoresponse reaches its peak amplitude and then attenuates towards the steady state potential characteristic for that particular intensity level. The amount of response compression is proportional to the adapting background (Laughlin, 1989; Juusola, 1993). This nonlinearity is clearly seen with long contrast steps: light decrements elicited larger responses than equally large light increments (Fig. 2 *B*). The biphasic photoresponses to both light increments and decrements suggests a system with a negative feed-back mechanism inhibiting the responses (cf., Fuortes and Hodgkin, 1964; French, 1980*b*; Juusola, 1993).

Experiments with step stimuli indicated that the photoresponses were limited to a voltage range of ~60 mV. In the following we will consider how this highly regulated and limited potential range behaves under different adaptation conditions when stimulated by dynamic contrast stimuli.

Adaptational Changes of Signal and Noise in Time Domain

To find out how the photoreceptor performance changes with light adaptation, we stimulated photoreceptors with repeated sequences of pseudorandomly modulated light contrasts at different adapting backgrounds. Each nonaveraged sequence of recorded photoresponse contained both responses to the momentary change in light

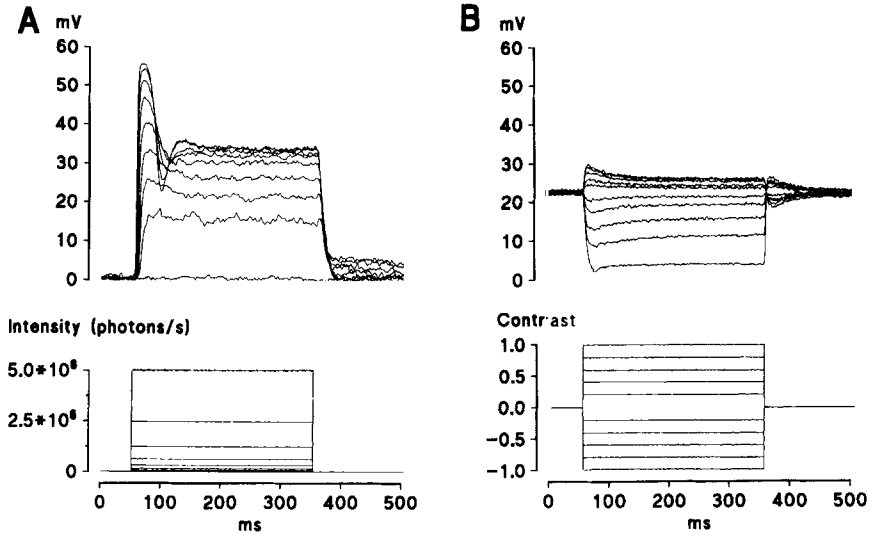

FIGURE 2. Intracellular recordings from the soma of a R1-6 photoreceptor, 0 mV denotes the dark resting potential (~ −60 mV). (*A*) Voltage responses of a dark adapted cell to 300 ms LED pulses with relative intensities 4, 8, 16, 32, 64, 128, 256, 1024, 2048 (2048 = $5.0 \cdot 10^6$ photons/s). Pulse interval 2 s, no averaging. (*B*) Voltage responses to 300-ms contrast step superimposed on the mean of $5.0 \cdot 10^5$ photons/s. Contrasts from −1 to +1 with a 0.2-s. interval. Each trace is five times averaged.

intensity, which we call the photoreceptor signal, and voltage noise. Noise is caused by the uncorrelated photon shot noise, intrinsic (transducer) noise, and dark noise (caused by membrane noise and, rare but possible, spontaneous bumps), in addition to the minor instrument noise (see also Lillywhite and Laughlin, 1979). To obtain a good estimate of the signal, the recorded sequences were averaged 30 times.

Fig. 3 *A* demonstrates samples of photoreceptor signals (i.e., averaged photoreceptor responses) to the identical sequence of pseudo-randomly modulated light intensity, with a mean contrast of 0.32 recorded at eight different adapting backgrounds. Two observations are evident: the more intense the adapting background, the more depolarized was the steady state potential and the larger the signal

superimposed on it. The increase in steady state potential and the variance of the photoreceptor signal are shown in Fig. 4*A* and *B*, respectively. The steady state depolarization, on which the actual contrast-induced photoresponses were superimposed, followed the well-known sigmoidal dependence on the adapting background

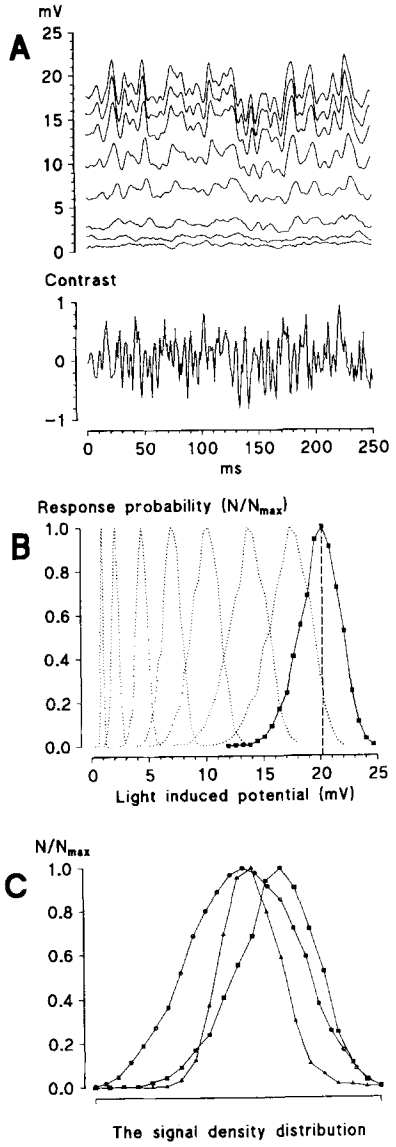

FIGURE 3. Dynamic characteristics of the averaged photoreceptor contrast response, i.e., the signal. (*A*) 250-ms samples of the averaged voltage responses (*top*) to the same sequence of the pseudorandomly modulated contrast stimulus (*bottom*) with a mean contrast of 0.32 superimposed on eight different adapting backgrounds, each 0.5-log intensity units apart. (*B*) The probability distribution of the response amplitudes at different adapting backgrounds, 0 mV denotes the dark resting potential. (*C*) A comparison of the response probability at low and high background with the Gaussian distribution of the contrast stimulus (*filled diamonds*, low background; *filled squares, high background; circles*, input signal).

intensity (e.g., Laughlin and Hardie, 1978). Thus, the steady state potential—set by adaptation—represents a static nonlinearity in phototransduction. The highest adapting background ($5.0 \cdot 10^5$ effective photons/s) depolarized the photoreceptor membrane by 21.0 ± 2.5 mV (mean of 11 cells ± SD). The variance of the

photoreceptor signal increased approximately log-linearly from the adapting background of $1.5 - 10^4$ effective photons/s onwards. Interestingly, the shape of its amplitude distribution (probability density function, or PDF) changed significantly as a function of light adaptation. The PDFs in Fig. 3 *B* illustrate this behavior, which is also a nonlinearity. At low adapting backgrounds up to ~ 5–10^3 effective photons/s the photoreceptors produced equally large depolarizations and hyperpolarizations.

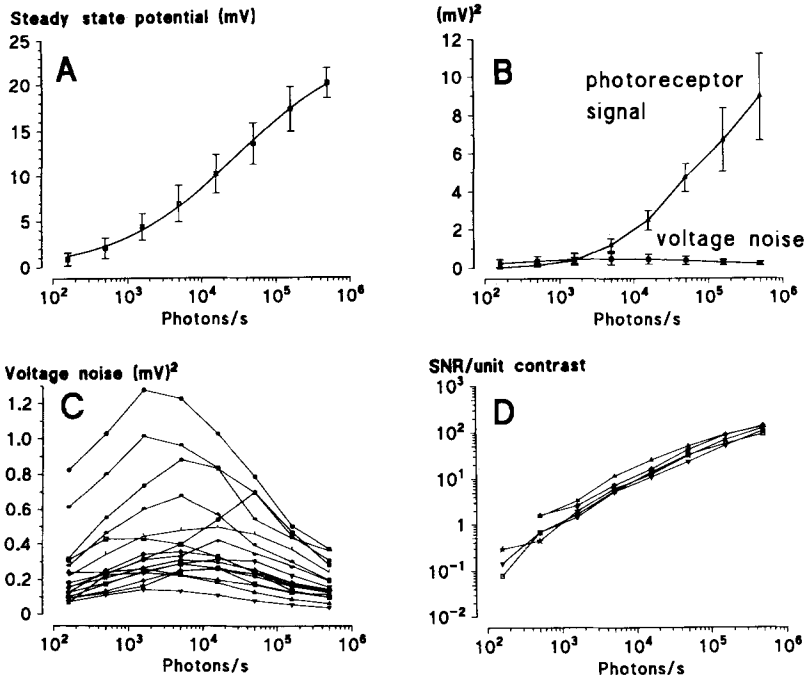

FIGURE 4. Light adaptational changes in the photoreceptor responses. (*A*) The steady state potential as the function of the background which follows a sigmoidal curve, 0 mV is the dark resting potential. Curve fitted with the self-shunting model ($V/V_{max} = RI^n/(RI^n + 1)$, V_{max} is the maximum response, R is the reciprocal of the intensity that induced the half-maximum voltage, n is an empirical exponent; see e.g., Laughlin and Hardie, 1978); mean of 17 cells, bars represent the SD. (*B*) The variance of a photoreceptor signal elicited by a mean contrast of 0.32 at different adapting backgrounds compared to the variance of background induced voltage noise. ($mean_{signal}$ of 5 and $mean_{noise}$ of 17 cells; ±SD). (*C*) The voltage noise at different adapting backgrounds for the 17 cells. Note the differences in the noise level between different photoreceptors. (*D*) Photoreceptor signal-to-noise ratio at different adapting backgrounds. The photoreceptor performance improves monotonically towards higher backgrounds.

Consequently, the amplitude distribution of the photoreceptor signal was Gaussian (Fig. 3 *B*) like the stimulus distribution. But as the light background was increased, the photoreceptor began to produce larger hyperpolarizations than depolarizations to the equal but opposite contrast stimuli, producing skewed distributions. This is shown in Fig. 3 *C*, which compares the Gaussian contrast input to the increasingly skewed amplitude distribution of the photoreceptor signals. This effect, which scales

the signals in favor of increasing hyperpolarizations is related to the attenuation of the driving force (E_l-E_m) as the membrane potential (E_m) reaches the reversal potential of the light induced current (E_l) (i.e., shelf-shunting compression; see Laughlin, 1989; Juusola, 1993) and to the increased probability of light-gated channel openings that cause the depolarization (see Hille, 1992, p. 323).

The variance of the background-induced noise had a maximum value of 0.32 ± 0.18 mV^2 (mean ± SD; $n = 11$) at an adapting background of ~5–10^3 photons/s (Fig. 4 *B*). There was a broad range of noise variance between cells, evidently related to their sensitivity differences, but in all cases the variance of the voltage noise decreased as the adapting background was increased further (Fig. 4 *C*). These observations are in accordance with previous voltage noise experiments in flies (Smola, 1976; Wu and Pak, 1978; Howard et al., 1987; Suss-Toby et al., 1991).

By dividing the variance of the photoreceptor signal (normalized to unit contrast) by the noise variance (induced by the corresponding background) we obtained the photoreceptor SNR, which is a direct measure of the effective amplitude of the noise (Laughlin, 1989). By using spectrally white pseudorandom modulation as a stimulus, the SNR is effectively weighted by the frequency response of the photoreceptor (Kouvalainen et al., 1993). The increase in signal variance and decrease in the noise caused the SNR to improve drastically as the adapting background was increased (Fig. 4 *D*). However, due to the limited intensity range of our light source (LED) we could not saturate the adaptational increase of signal variance. Further, it must be emphasized that the value of the SNR normalized to unit contrast depends on the applied stimuli (Juusola, 1993). This is because of compressive nonlinearities like self-shunting, whose effect increases with increasing depolarizations, so that the smaller the contrast, the larger would be the normalized SNR value. This is particularly true with the contrast step approach, where the peak response is often the only parameter used as the signal (Juusola, 1993). Although, in case of a pseudorandom stimulus, as seen with the skewed probability density histograms in Fig. 3 *B*, the averaging changes in depolarizing and hyperpolarizing responses reduce this effect, the superposition principle is valid for each stimulus only (see below the linearization by white-noise stimulus). Our results are roughly in agreement with the SNR values of Howard et al. (1987) who used small depolarizing contrast steps (see also Howard and Snyder, 1983).

Power Spectra of Noise and Contrast Signal

If the contrast stimulus adds noise to the photoresponse, then the total noise spectrum (i.e., containing both background noise and any additional noise produced by the modulation) should differ from the noise spectrum induced by the same background alone. Fig. 5 *A* shows an example of how the total noise was derived from the recordings and compares the total noise in the time domain to a corresponding sample of the background-induced noise. These noise levels are virtually indistinguishable. Fig. 5 *B* shows two samples of both the background and the total noise power spectra. It is clear that, regardless of the adapting background used or the magnitude of the mean contrast, we could not separate the contrast-induced noise from the noise induced by the same background. This indicates that no additional noise is elicited by contrast in a light adapted photoreceptor stimulation.

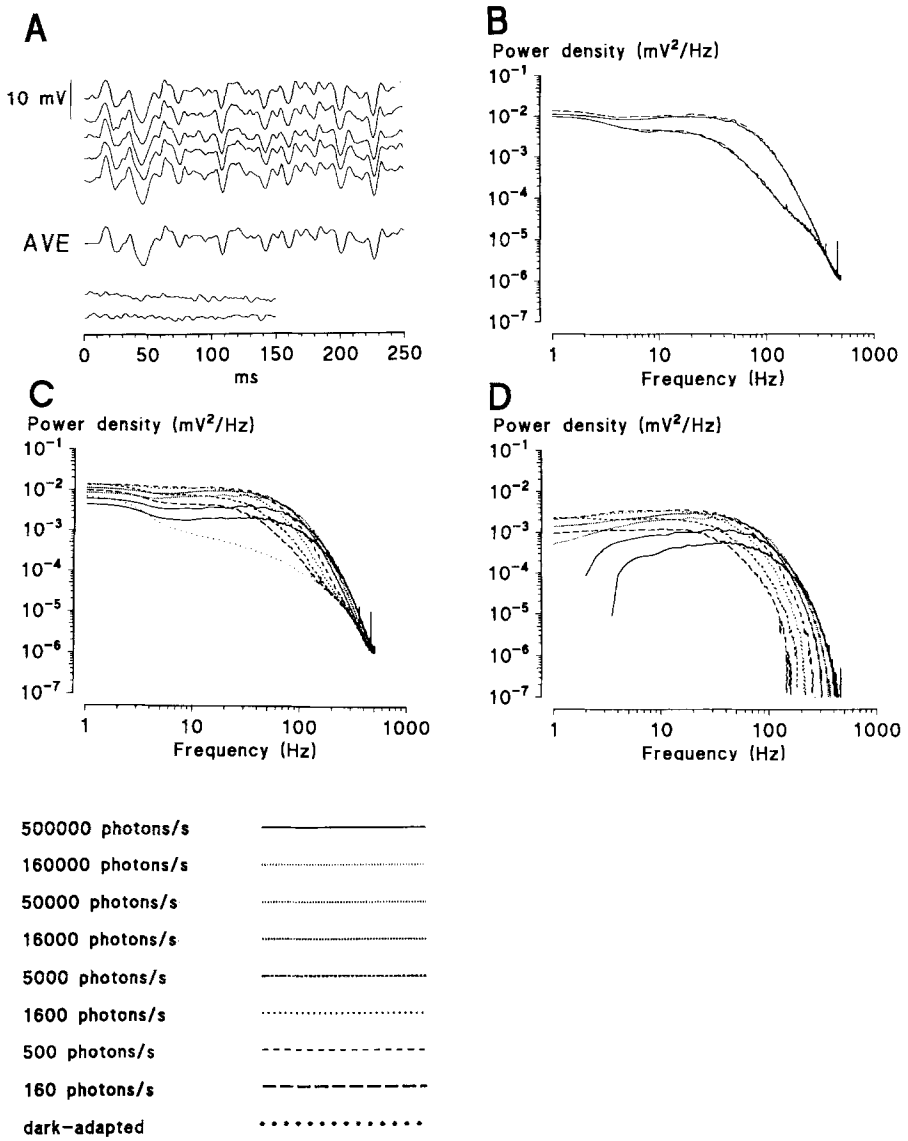

FIGURE 5. Analysis of photoreceptor noise at different adapting backgrounds. (*A*) Five samples of nonaveraged photoreceptor responses (*top five traces*) and the averaged response (AVE) to a contrast of 0.32 recorded at the adapting background of $5.0 \cdot 10^5$ photons/s. As an example the averaged response is subtracted from the third nonaveraged response and the result, the contrast induced noise (*second lowest*), is compared to the noise induced by the background (*bottom trace*). (*B*) Comparison between the power spectra of the signal-induced noise (*discontinuous line*) and background-induced noise (*continuous line*) showed that they did not differ significantly. The extremely small differences in the power can be explained by the roughness of the estimates. (*C*) The power spectra of signal induced noise in dark and at eight different adapting backgrounds. (*D*) The power spectra of transducer noise calculated by subtracting the dark noise spectrum from each signal-induced noise spectrum. Below the figures is the line decoder for the various line types and corresponding light backgrounds. This decoder applies to all subsequent figures with varied background.

Fig. 5 *C* illustrates the power spectra of the total noise generated by 0.32 contrast stimulus at eight different adapting backgrounds, together with the dark noise power spectrum. The total noise did not differ from the noise induced by analogous backgrounds, which therefore gave exactly the same results with the contrasts used here. By subtracting the dark noise spectrum from each total noise spectrum we obtained the averaged power spectra of the light-induced noise (Fig. 5 *D*). At higher adapting backgrounds a greater proportion of the power lay at higher frequencies, so that the high frequency end extended further and the low frequency end was attenuated as the background was intensified. This implies adaptational changes in bump size, shape and duration, as reported before (Wong, Knight, and Dodge, 1982). Indeed, these changes in the bump parameters are further augmented by self-shunting and a voltage-dependent membrane (Juusola and Weckström, 1993) which modulate the light-induced current in the same direction (see Discussion).

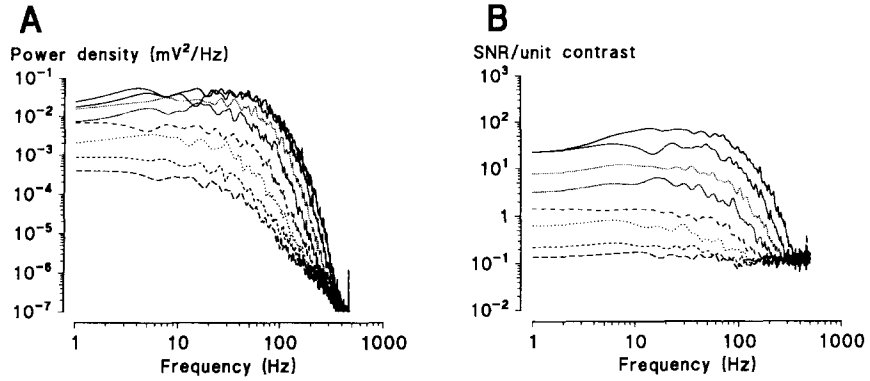

FIGURE 6. Photoreceptor signal power spectra, *A*, and the frequency domain presentation of the photoreceptor signal-to-noise ratio, *B*, at eight different adapting backgrounds. The power of the photoreceptor signal (elicited by 0.32 mean contrast) increases and shifts towards high frequencies as the background is increased. At low adapting background the signal power spectra are very much like the corresponding noise spectra (compare with Fig. 7 *B*). The photoreceptor signal-to-noise ratio improved drastically towards high frequencies at high backgrounds.

Signal power spectra were calculated from the pseudorandomly modulated contrast signal superimposed on the adapting backgrounds (Fig. 6 *A*). At low adapting backgrounds, the photoreceptor signal spectra resembled the corresponding noise. This is because of the small signal amplitude which, regardless of averaging, was not large enough to be fully separated from noise. The adaptational increase of the photoreceptor signal seen in Fig. 4 *B* was mainly caused by the increased contrast gain (see below) which shifted the power towards high frequencies. The concomitant improvement of the photoreceptor SNR at high frequencies is seen well in Fig. 6 *B*.

Adaptational Changes of the Frequency Responses

The frequency response recordings were generally stable for a considerable period and on four occasions a complete contrast recording series was obtained from a

single photoreceptor cell. However, time domain averaging drastically improved the SNR when using low contrast stimulation. It must be pointed out here that, because of the time domain averaging, the calculated frequency response functions per se do not tell us whether the animal can detect the contrast changes in a given photoreceptor output. But they do tell us of the ability of the photoreceptor to perform transduction, its speed and contrast gain, however small the signals generated. The frequency responses, being the actual ratios between the contrast stimuli and the voltage responses produced, provide us with information about the photoreceptor transfer characteristics. The gain part of this input-output relation demonstrates the ability of a photoreceptor to amplify each frequency of the contrast stimulus and the phase part gives us information on how much the responses lag behind a particular frequency in the stimulus used.

Fig. 7 illustrates the gain functions of the photoreceptor frequency responses at eight different adapting backgrounds scaled by the numbers of effective photons per second. The adaptational loss of sensitivity is seen as a reduction in gain. This is because at low adapting backgrounds the bumps are larger and slower than the ones induced by higher adapting backgrounds (Wong et al., 1982). However, when the

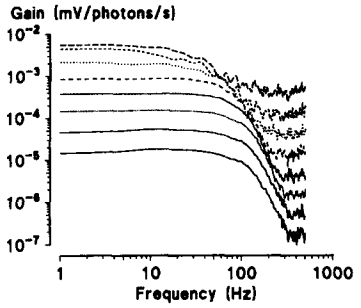

FIGURE 7. The gain part of the photoreceptor frequency response scaled by the number of effective photons/s (i.e., sensitivity). The upper trace is the gain at the lowest adapting background, whereas the lowest trace shows the gain at the highest tested adapting background. Note how the photoreceptor sensitivity decreased along with adaptation.

same experiment was scaled as [mV/unit contrast], the photoreceptor contrast gain (calculated as the photoreceptor response divided by stimulus contrast; Shapley and Enroth-Cugell, 1984) increased along with the adapting background (Fig. 8 *A*) up to $\sim 2 \cdot 10^5$ photons/s before beginning to saturate. Simultaneously the 3 dB cut-off frequency (Fig. 9 *A*) shifted from ~20 Hz with the lowest background to a saturated value of about 60 Hz at about $2.0 \cdot 10^4$ photons/s. The gain functions were best fitted by two resonances and one double pole (see Appendix). The only real discrepancy between the fitted functions and the experimentally derived gains was the slight attenuation of the low frequency end of the two highest adapting backgrounds.

Fig. 8 *C* shows photoreceptor coherence functions at eight different adapting backgrounds with 0.32 contrast. The linear transduction properties described here confirm the results of earlier studies conducted at a constant adapting background (Pinter, 1966; Leutscher-Hazelhoff, 1975; French, 1980*b*,*c*; Weckström et al., 1988). Even at weak adapting backgrounds (about $5 - 10^3$ photons/s) photoreceptors demonstrate a high degree of linearity (coherence > 0.9) in the frequency range from 10–100 Hz (Fig. 8 *C*). Indeed, the improved coherence at high backgrounds

indicates that the linearity of R1-six photoreceptors does not diminish with light adaptation (see also Pinter, 1966, 1972; Leutscher-Hazelhoff, 1975).

The R1-6 photoreceptor response lagged behind the contrast stimulus by an amount depending on the cell's adaptational state (Fig. 8 *B*). The more intense the adapting background the less the lag. At the moderately dim adapting background of 1600 photons/s the photoreceptor phase lag was more than −450 degrees at 90 Hz (Fig. 9 *B*). As the background increased to $\sim 5 \cdot 10^5$ photons/s, the phase at the same frequency decreased by more than 250°. From 1 Hz upwards, the photoreceptor

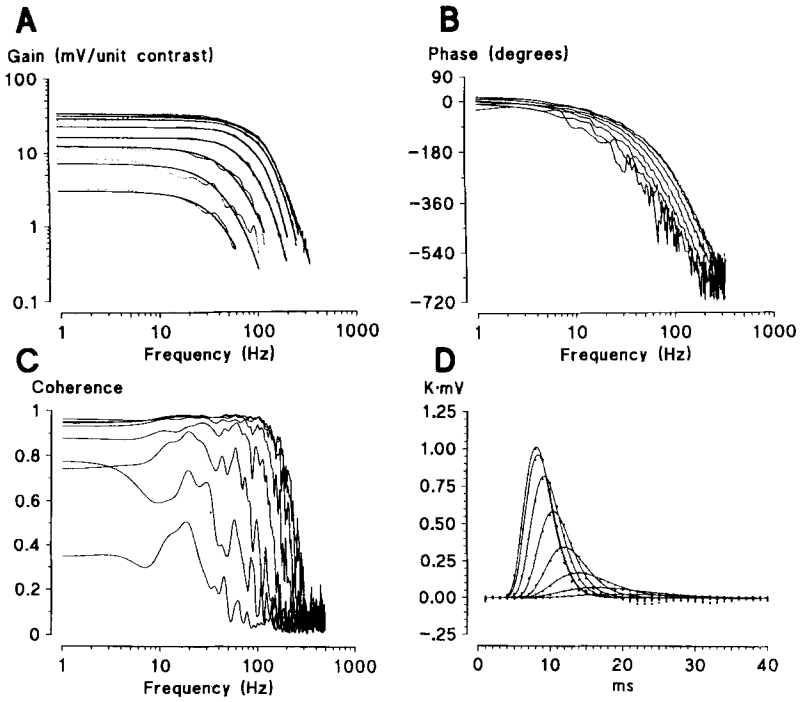

FIGURE 8. Analysis of the photoreceptor frequency response at different adapting backgrounds calculated from the mean contrast stimulus of 0.32 and the photoreceptor voltage responses. (*A*) The photoreceptor contrast gain. (*B*) The corresponding phase functions. The photoreceptor phase speeds up in light adaptation towards the high frequencies. (*C*) The coherence function that is a measure of the photoreceptor's linearity. (*D*) The linear impulse responses calculated by inverse FFT.

phase functions of consecutive backgrounds maintained a monotonic increase in mutual distance up to ~200 Hz. At still higher frequencies, the decline of the SNR (as seen in the near zero coherence in Fig. 8 *C*) made reliable phase estimates impossible.

The effect of increasing adapting background on transduction speed was also clearly seen in the first order kernels of the photoreceptor responses (Fig. 8 *D*). With increasing background, but the same contrast, the amplitude of the calculated kernels increased while the latency and the total duration were reduced (see also

Dubs, 1981; Howard, Dubs, and Payne, 1984). The kernels were relatively well-fitted by a log-normal function as suggested by Howard et al. (1984). However, as the gain of the frequency response calculated from the fitted kernels did not fit the resonances in the experimental gain, the log-normal function was not used to fit the gains (see Appendix).

The results of using different mean contrasts at the same adapting background are shown in Fig. 10. The unit contrast gain of a photoreceptor decreased with the increased stimulus (Fig. 10 *A*), as found recently with different contrast pulse stimuli (Juusola, 1993). However, regardless of the mean contrast applied, the characteristic shapes of the gain functions in different R1-6 photoreceptors stayed unchanged when recorded at the same adapting background. Only the variance of the gain estimates grew smaller as the increased contrast stimulus magnified the photorecep-

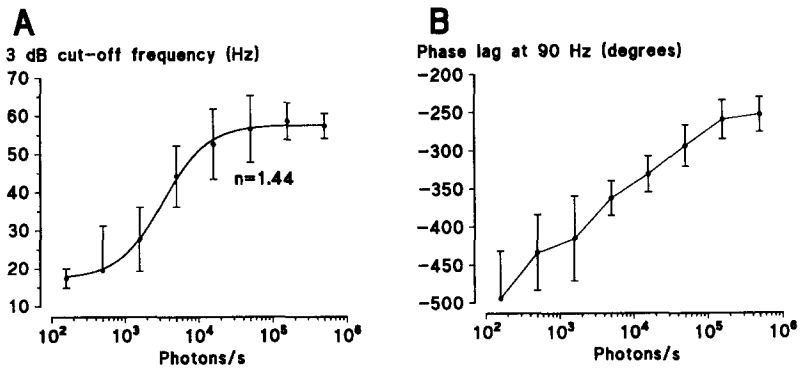

FIGURE 9. Adaptational changes in the 3 dB cut-off frequency and in the phase lag (mean of four cells ± SD). (*A*) The 3 dB cut-off frequency had a steep increase between backgrounds of 10^3 and 10^4 photons/s before saturating to ~65 Hz. (*B*) The phase lag demonstrated attenuation throughout the increased light adaptation range. At the highest adapting background the photoreceptor response to a mean contrast stimulus at 90 Hz lagged ~250° behind the stimulus.

tor voltage signal. The characteristic form of the photoreceptor gain estimate was preserved from mean contrasts as low as 0.04 up to the highest tested, 1.80 (not shown, tested with an external random signal generator). The increasing response compression caused by the increasing mean contrast is clearly seen in the first order kernels (Fig. 10 *D*) scaled to the unit contrast.

We found no evidence that either increase or decrease of mean contrast could alter the phase of a photoreceptor soma's frequency response at a given background (Fig. 10 *B*). This means that the mean adapting background determines the photoreceptor phase. Accordingly, when we compared the time courses of the first order kernels obtained with stimuli of different contrast at a given adapting background, we could not see any obvious changes in transduction speed. With an adapting background of 5.0–10^5 effective photons/s (Fig. 10 *D*), the 1st order kernels with 0.42 and 0.04 mean contrast stimuli reached their peak responses simultaneously.

The responses to pseudorandomly modulated stimulation indicated a highly linear phototransduction system, which was supported by the coherence functions (Figs. 8 *C* and 10 *C*). Contrary to expectations, the greater the applied mean contrast, the more linear were the responses, as judged by the coherence function estimates. Thus, the coherence stayed between 0.90–0.99 (from 1 to 150 Hz). This latter finding is

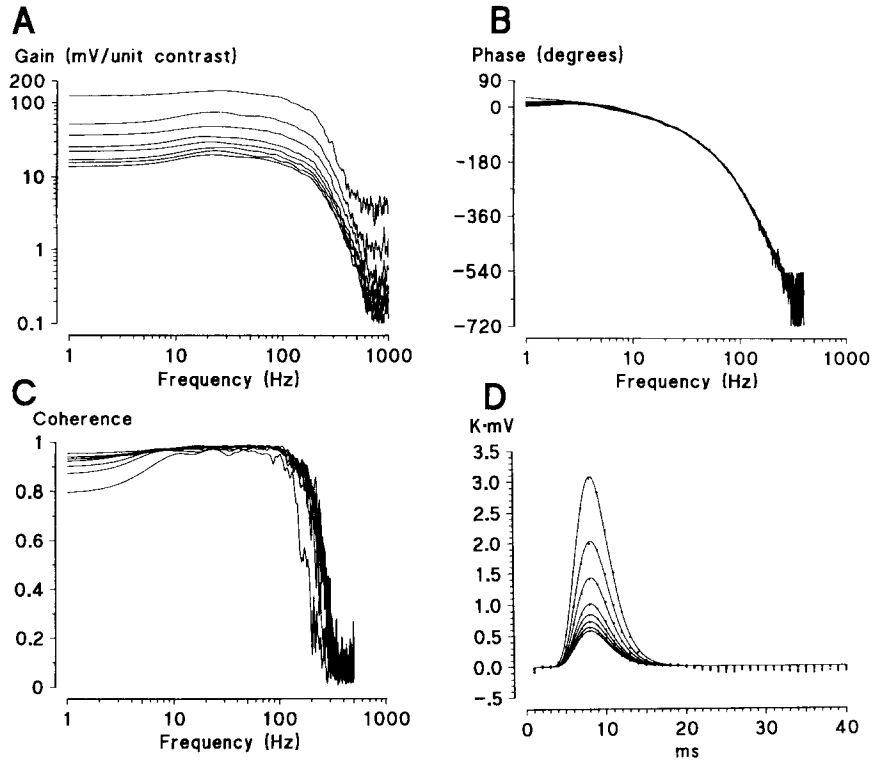

FIGURE 10. Photoreceptor frequency responses at the adapting background of $5.0 \cdot 10^5$ photons/s calculated from different mean contrast stimulus of 0.09, 0.17, 0.25, 0.32, 0.36, 0.38, 0.40, 0.42 and the corresponding photoreceptor voltage responses. (*A*) The decrease in the contrast gain as the mean contrast is increased. The topmost trace was obtained with the smallest and the lowest with the largest contrast. (*B*) The corresponding phase functions which were independent of the contrast modification. Hence the photoreceptor phase was posited by the adapting background. (*C*) The corresponding coherence functions. The greater was the mean contrast the more linear was the photoreceptor function. (*D*) The linear impulse responses calculated via inverse FFT reached their peak amplitudes exactly at the same time, but their amplitude decreased as expected on basis of the gain function.

obviously related to the increase in SNR, as shown in the frequency domain in Fig. 6 *B*, and not to changes in the linearity of the system. It should be remembered that the coherence function measures both SNR and nonlinearities. When the contrast modulation increases, the signal amplitude increases, but the noise level is unchanged. Hence, we see an improvement in the coherence value. Although the

largest mean contrasts also included intensity changes, which more than doubled the mean illumination and elicited responses with peak-to-peak amplitudes up to 20–30 mV, they did not reduce the linearity of the system.

Dead Time

The phase of a minimum phase linear system can be derived directly from the gain function (Bendat and Piersol, 1971). Such a system has no dead time, or pure time

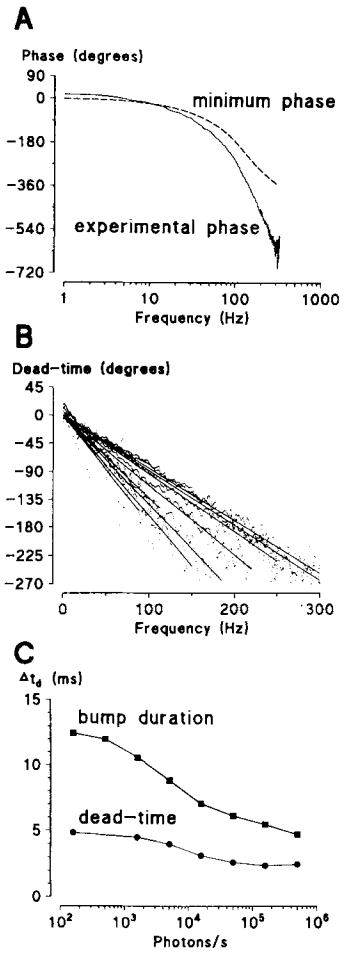

FIGURE 11. Photoreceptor dead-time (or pure time delay) at different adapting backgrounds. (*A*) The minimum phase, calculated from the fitted gain function (*dashed line*) and compared to the phase function calculated from the input and output data (*continuous line*). (*B*) The difference between the phases as depicted in *A*, i.e., the dead time, at different adapting backgrounds (note the linear frequency scale). The dead time decreases linearly as a function of frequency. (*C*) The dead time and the bump duration (calculated by Eq. 6 from the data in Fig. 5 *D*) at different adapting backgrounds. The dead time decreases in light adaptation parallel with the decrease of the bump duration.

delay (see also Methods). Insect photoreceptors are not minimum phase systems, as shown previously by French (1980*b*,*c*). The phases calculated on the basis of the fitted gain functions (that may be called gain-dependent, see Appendix) differed from the phases of the experimentally derived frequency responses. Fig. 11 *A* compares the phase of a photoresponse recorded at an adapting background of $5.0 \cdot 10^5$ photons/s with the minimum phase calculated from the corresponding gain function. The photoreceptor phase led the minimum phase up to ~ 10 Hz (cf., Weckström et

al., 1988), but then lagged behind the minimum phase. The dead time in phototransduction is the slope of the difference between the minimum phase and the experimental phase (Fig. 11 *B*).

Surprisingly, we found that the dead time, in addition to the gain-dependent delay, was reduced by light adaptation (Figs. 11, *B* and *C*), corresponding to an adaptational acceleration of the photoresponse. The 5-ms dead time in phototransduction at low adapting backgrounds was reduced to a saturated minimum of 2.5 ms at a moderately high adapting background of $\sim 1.0 \cdot 10^5$ effective photons/s. Interestingly, the dead time changed in parallel with the corresponding bump duration calculated from the noise power spectra (see Methods) when the photoreceptor was light adapted (Fig. 11 *C*) (cf., Howard et al., 1987; Roebroek et al., 1990).

DISCUSSION

We have demonstrated the ability of light adapted fly photoreceptors to maintain a linear performance when stimulated by a variety of contrasts. We will argue that this results from the high early gain of the receptors followed by delayed compressive feedbacks. These adaptation processes, although nonlinear, allow the phototransduction mechanism to produce a linear input-output relationship. The linearity of phototransduction has been pointed out by other investigators (Leutzer-Hazelhoff, 1975; French 1980*a,b*; Weckström et al., 1988) and contrast coding has been investigated quite extensively with step stimuli by Howard and co-workers (1987) and by Juusola (1993). However, the results obtained here are unique in showing how well linearity is conserved in light-adapted photoreceptors, how the SNR behaves as a function of stimulus frequency, and how the pure time delay (dead time) of phototransduction is changed by light adaptation.

Recent advances in our understanding of invertebrate phototransduction (Fein, Payne, Corson, Berridge and Irvine, 1984; Brown et al., 1984; Fein and Payne, 1989; Hardie, 1991; Hardie and Minke, 1992; Nagy, 1991; Minke and Selinger, 1988) point to an Ins(1-4-5)P_3-mediated molecular mechanism being responsible for excitation in photoreceptors. According to this scheme, the excited rhodopsin molecules in microvillar membranes trigger Ca^{2+}-release from internal stores close to the base of the microvilli. This calcium then opens cation channels that, in the fly, seem to be permeable mainly to calcium but also partly to sodium (Hardie, 1991; Hardie and Minke, 1992). We will consider the dynamic linearity of the photoreceptor transduction in this context, taking into account two other lines of investigation, namely the control of contrast gain in photoreceptors (see e.g., Shapley and Enroth-Cugell, 1984; Laughlin 1981, 1989; Juusola, 1993) and photoreceptor membrane properties (Laughlin and Weckström, 1989; Weckström et al., 1991; Juusola and Weckström, 1993).

Evidence for a High Degree of Linearity

The linearity of phototransduction was examined by calculating the coherence function (Figs. 8 *C* and 10 *C*). If coherence is close to unity, the overall behavior is linear and free of noise. In the present study, we found that regardless of the stimulus contrast, the system was linear in the frequency range 10–150 Hz; specifically, this

was true with all tested adapting backgrounds of more than ~5000 photons/s. Coherence estimates yielding smaller values, at lower backgrounds and at frequencies higher than 150 Hz, were caused by the poor SNR (compare Fig. 8 *C* with Fig. 10 *C*). We could improve the photoreceptor coherence estimates at low backgrounds by increasing the number of averages, but because of the low-pass frequency responses, this procedure only slightly improved the coherence at high frequencies. At low frequencies, below 10 Hz, the coherence dropped slightly at high backgrounds. This was reported earlier by Weckström et al. (1988) who called it phase-lead nonlinearity. It is caused by adaptation of the photoresponse to a slowly changing stimulus. At 1 Hz and below, the light response becomes clearly nonlinear because of the same light adaptation processes that control the overall gain of the system. However, in the behaviorally important range of frequencies, fly phototransduction produces voltage responses that depend linearly on the momentary change of stimulus intensity. Even very large stimulus modulation (with the contrast of 1.8) did not decrease the linearity. These findings were unexpected, considering the nonlinearity of photoresponses obtained with simple sinusoidal stimuli (Pinter, 1966; Leutscher-Hazelhoff, 1975; Weckström et al., 1988).

What is the functional basis for this kind of linear contrast coding in the fly photoreceptors? Blowfly photoresponses demonstrate an adaptive regulation that is characteristic of feed-back: step responses and first order kernels show over- and undershoots during and after the light stimulus (Figs. 2, 8, and 10) and the frequency responses can only be modeled by including second order poles into the system. The visual system of a blowfly has evolved to function best in its natural surroundings, and the adaptive properties of its visual system are matched to detect contrast changes even in fast movements like flying. The Gaussian contrast stimulus we used was probably rich enough to mimic the frequency and amplitude variations which a flying fly may experience (Fig. 1). To obtain reliable images from its natural surroundings during fast motion, the light-adapted visual system of a fly has to rapidly and efficiently detect both incremental and decremental contrast changes. Because of the optical blur (Laughlin, 1989) and the transduction noise (Figs. 4 *C* and 5), the phototransduction gain must produce a high SNR (Figs. 4 *D* and 6 *B*).

We propose that the linear photoreceptor performance is a result of combining fast amplification in the early response generation with a slightly delayed compressive feedback mechanisms set by the previous output to keep the system in a suitable state for the most probable input signal. When a photoreceptor is adapted to a given background, and the light intensity does not change or changes slower than the action of the previously set feedback, compressive nonlinearities will dominate (cf., positive and negative contrast responses in Fig. 2 *B*; Juusola, 1993; French, Korenberg, Järvilehto, Kouvalainen, Juusola, and Weckström, 1993). However, if a transient stimulus is superimposed on a slower change in light intensity, the dynamically modulated gain linearises the photoresponses (cf., Leutscher-Hazelhoff, 1975). Thus, the crucial point is the speed of the feed-back; under dynamic stimulation conditions only slow frequencies create nonlinearities, seen as a drop in the coherence at frequencies below 10 Hz. It has been shown previously that in nonlinearities of the rectifying type, like light-adaptation, the addition of noncorrelated signals (i.e.,

noise) tends to linearize the system (Spekreijse and van der Tweel, 1965; Spekreijse and Oostings, 1970; French et al., 1972).

How Is Photoreceptor Contrast Gain Regulated?

A photoreceptor produces an elementary response from each absorbed photon (in locust: Lillywhite, 1977; in *Limulus*: Wong, 1978; Wong et al., 1982; in fly: Wu and Pak, 1978; Suss-Toby et al., 1991). Because the response generation is a process with a limited number of available transduction units (Howard et al., 1987), its output depends on the rate at which effective photons enter the eye (i.e., the contrast stimulus duration) and on the speed of adaptation (i.e., gain control) (Juusola, 1993). When the photon flow is changing dynamically, not only the number and shape of the bumps contributing to the photoresponse, but also their duration and latency is constantly changing. Recent studies suggest that these effects are caused by regulation of intracellular Ca^{2+} concentration (Payne, Walz, Levy, and Fein, 1988; Payne, Flores, and Fein, 1990; Hardie, 1991; Hardie and Minke, 1992) which is further augmented by self-shunting (Laughlin, 1989; Juusola, 1993) and by increased activation of voltage sensitive potassium channels (Laughlin and Weckström, 1989; Weckström et al., 1991; Juusola and Weckström, 1993).

Hardie (1991) demonstrated a positive feedback by Ca^{2+} enhancing the light current. However, the positive Ca^{2+} feed-back acts sequentially with a negative feedback reducing the calcium influx through light-activated channels, because the positive feedback is slightly faster. One factor in this system could be the cooperativity of light-gated channels. Hardie (1991) estimated that four Ca^{2+} binding sites for the internal transmitter have to be filled before the light gated channels in *Drosophila* can open. In *Limulus* a similar type of cooperativity at light-gated channels has been suggested to cause the high early gain (cf., "bump specks" proposed by Stieve, Schnagenberg, Huhn, and Reuss, 1986). However, according to Payne, Corson, Fein, and Berridge (1986) the Ca^{2+} concentration would be diluted quickly as Ca^{2+} has greater affinity for other buffering proteins than channel binding sites. Indeed, Ca^{2+} has a negative feedback effect on its own release from the submicrovillar stores (Payne et al., 1988, 1990). Thus, the mean number of effective photons entering the photoreceptor regulates the average intracellular Ca^{2+} level via a complex machinery. How do our results relate to these questions?

The speeding up of phototransduction by negative feed-back from increased intracellular Ca^{2+} and a voltage-dependent membrane are probably the major adaptive mechanisms contributing to the increasing acceleration of the photoreceptor kinetics as a function of light adaptation. Increasing light adaptation generates faster responses, which is evident from the gain and the phase of the transfer function (Figs. 8 *B*, 9 *A*, and 9 *B*). The acceleration of phototransduction, can also be seen in the first order kernels (impulse responses if a linear system) calculated from the transfer functions via the inverse FFT (Fig. 8 *D*). Interestingly, the size of the contrast stimulus did not have any effect on the photoresponse phase nor on their time-to-peak values (Figs. 10 *B* and *D*). Thus, the mean adapting background determines the speed of the photoresponse, as expected on the basis of a combined action of a voltage-dependent membrane and Ca^{2+} regulation.

Dead Time, Bump Duration and Speed of Adaptation

Previously it was shown (Howard et al., 1987; Roebroek et al., 1990) that average bump duration can decrease from ~20 ms in darkness to ~2 ms in full daylight. In the present work we found that the dead time in phototransduction was also reduced along with the shortening of the bump duration (Fig. 11 *B* and *C*). The dead time (or pure time delay) seems unlikely to arise from enzymatic reactions or normal diffusion, but requires queuing or threshold phenomena (see discussion in French, 1980*c*), suggesting that the dead time and the bump duration could have different origins. However, it may still be advantageous for the two parameters to be matched. If the dead time and bump duration are related, we can think of three possible mechanistic explanations for their correlation.

The first hypothesis is a simple queuing mechanism. Then the time needed to deliver a burst of transmitter through a microvillar queue would be set by the bump duration. A second possibility is that one microvillus could produce only one burst of internal transmitter at a time and, before its delivery, initiation of the next burst is impossible, regardless of the number of photons absorbed by the microvillus. This explanation requires some additional assumptions, because something must be causing the refractory period in the microvillus. The limit of bump duration would be set by consecutive transmitter bursts and this would represent the dead-time.

The third and most likely explanation is based on the recent finding in *Xenopus* oocytes that Ca^{2+} enhanced release of Ca^{2+} from intracellular stores occurs in an all-or-none fashion after its initiation by bursts of Ins(1-4-5)P_3 (Lechleiter and Clapham, 1992). This would lead to a dead time because there is a threshold for Ca^{2+}-release. The same studies showed that intracellular release forms distinct waves, and if such waves meet each other, they are annihilated. This kind of behavior in photoreceptors would explain the reduction of light-gated channels activated per absorbed photon from many to one as the photoreceptor is light adapted.

How do these hypotheses fit with the data? In the present study the first order kernels reached their peak values in 10 ms at a moderately high adapting background of $5.0 \cdot 10^5$ effective photons/s regardless of the mean contrast (Fig. 10 *D*). This is in agreement with Juusola (1993) who found that at the same background with the rising phase of the photoresponses stayed unchanged during the first 10 ms regardless of the duration of the contrast step. There, a 2-ms lasting contrast step was needed to elicit a response that reached its peak amplitude in 10 ms, whereas any longer contrast steps produced nonlinearly amplified peak responses. Again, these findings relate the linearity of the photoresponses to the speed of adaptation. They suggest that it takes at least 2 ms of constant stimulation before the adaptive mechanisms can change bump summation. Therefore, after initiation of the stimulus inhibition starts only after a delay, whose magnitude may depend on the dead-time in bump production (see also Payne et al., 1988; Payne et al., 1990). Hence, when the intensity is changed, the high early gain of the responses bypasses the following feedback compression and sums up to form a linear photoresponse.

How Is the Linearity of the Voltage-dependent Photoreceptor Membrane Achieved?

The steady state potential as a function of adapting light intensity follows a sigmoidal curve saturating between 15 and 30 mV above the resting potential. In our

experiments, the maximum was 23 mV on average (Fig. 4 *A*). This saturation limit is a balance between the maximum number of depolarizing (light-activated) and hyperpolarizing (voltage-activated) conductances at this membrane voltage. Opening channels significantly lowers the membrane time constant, nearly 10-fold by a 20-mV depolarization (Weckström et al., 1991; Juusola and Weckström, 1993). Thus, the membrane allows faster voltage signals at the cost of a higher driving current and gain reduction. However, the membrane voltage still lies in a range where the voltage-dependent potassium channels are continuously activating and relaxing as the membrane voltage is changed by light (Juusola and Weckström, 1993). This voltage-dependent membrane conductance becomes approximately linear above the resting potential (Juusola and Weckström, 1993). In addition, the activation and relaxation time constants of the potassium channels are accurately matched at light-adapted membrane potentials (see also Weckström et al., 1991). This means that the photoreceptor membrane rectifies in both directions, outwardly when more channels are being activated and inwardly when more channels are being closed. This rectification produces quite symmetric voltage changes in response to current steps of opposite polarity in light-adapted potentials, although less so near the resting potential. With increasing depolarizations the photoreceptor membrane, a low-pass filter in the dark, acquires more and more band-pass characteristics. Although the membrane behaves nonlinearly near the resting potential, it is linear when light adapted and therefore depolarized.

Reduction of Sensitivity Is Necessary for Maximum Contrast Gain and High SNR

Light adaptation reduces the sensitivity of photoreceptors (Fig. 7, also in *Limulus*: Fuortes and Hodgkin, 1964; in blowfly: Zettler, 1969; Laughlin and Hardie, 1978; Howard et al., 1984). How is this to be interpreted in terms of light adaptational increase in contrast gain?

A basic problem in all sensory transduction is to accomplish a maximum response amplification while suppressing noise. Changing sensitivity is an elegant way to deal with this problem. As the ambient light increases, the amount of light reflected from objects increases to the same extent, so that the contrasts between objects remain unchanged, but the number of photons being transduced is greater. To succeed in coding contrast while light intensity increases, photoreceptors have to continuously decrease their sensitivity to keep the signals of a few millivolts within the voltage limits of a linearized photoreceptor membrane. Hence, the higher the adapting background the smaller are the bumps generated, the greater number of them sum to form each photoresponse and the weaker is the background noise. For example, at the adapting background of $5.0 \cdot 10^5$ photons/s the photoresponses elicited by a contrast of 1 ($1.0 \cdot 10^6$ photons/s) provided a SNR of ~ 100 (Fig. 6). The effect of adaptational desensitation on the response also depends on the speed of changes in photon flow (i.e., the speed of the contrast change), because the feed-back inhibition will least influence the responses to transient contrast changes. In general, adaptation sets the contrast gain to the most sensitive range that does not saturate phototransduction. By desensitizing, or adapting, to different backgrounds photoreceptors can code the information about contrast relatively independently from absolute intensity.

There is variation among different species in how much the transduction machin-

ery can amplify the contrast input, and the range of adapting backgrounds for which the increase in amplification is extended before the contrast signals match the needs of an animal (cf., Howard et al., 1984; Laughlin and Weckström, 1993). In blowfly photoreceptors, moving from dark to moderate adapting backgrounds, the amplification of contrast signals is increased ~10-fold before it begins to saturate. This occurs near an adapting background of $1.7 \cdot 10^5$ photons/s (Fig. 10*A*). Howard et al. (1987) and Weckström et al. (1991) also found only a minor increase in the magnitude of voltage responses from adapting backgrounds of 5 log units onwards. However, despite the fact that the contrast responses do not increase beyond those backgrounds, the voltage noise still diminishes steadily as the bump amplitude is decreasing. This in turn improves the photoreceptor performance in terms of the SNR as the adapting background is increased. It seems evident that the shunting action of a light-induced current (with the help of the delayed rectifier) works efficiently near saturating steady state potentials, and thereby limits the contrast response from higher amplification. But, it should be remembered that the migration of the screening pigment begins to activate at the same adapting backgrounds where the steady-state voltage saturates (Stavenga, 1989; Roebroek and Stavenga, 1990). By pigment migration, fly photoreceptors avoid saturation of the limited number of transduction units (microvilli) available and broaden the intensity range with a high SNR (Howard et al., 1987).

Why Linear Responses?

The linearity of a sensor is useful in man-made measurement applications. In the case of the nervous system the advantages are not so obvious. The network following the light sensors could be well adapted to the nonlinear transformations that take place in the periphery. Still, it may be impossible to recover all of the information coded in the nonlinear processes in the photoreceptors. Therefore, we propose that the time during which the gain control in photoreceptors takes effect must be such that the natural stimuli do not normally change their shape or intensity because of this gain control. When the animal looks at moving objects or is itself moving (see e.g., Borst, 1990), it is conceivable that the gain control would not affect its detailed perception of the world. The high speed of the feed-back in photoreceptors means that the animal, or its field of view, must move from time to time to prevent the spatial contrasts from disappearing or dimming through adaptation. This is a well known phenomenon in the vertebrate eye relieved by ocular microsaccades. A similar system has been described in the fly compound eye, where several intracapsular muscles can force small saccades with a frequency of ~ 0.5–1 Hz (Hengstenberg, 1971; Franceschini, Chagneux, Kirschfeld, and Mücke, 1991). This is probably fast enough to prevent serious distortions in the animal's visual perception.

APPENDIX

Fitting the Frequency Responses

As the fitting of multiparameter nonlinear functions to any given experimental data is notoriously ill-conditioned, and prone to reflect the investigators (possibly biased) views, some detailed explanation is needed of how this was done in this work.

The photoreceptor frequency responses were assumed to result from a linear system with a general form for a minimum phase linear system

$$\frac{K \times \prod_{i=1}^{n} Z(\omega) \times \prod_{j=1}^{m} W(\omega)}{\prod_{k=1}^{l} P(\omega) \times \prod_{r=1}^{q} R(\omega)} \tag{7}$$

where K is a constant of proportionality, f is frequency, $Z(\omega)$ means zeroes of first order, $W(\omega)$ means zeroes of second order, $P(\omega)$ denotes poles of first order, and $R(\omega)$ stands for resonances or second order terms. As it is possible to fit arbitrarily complex fractionals to any given frequency response, the fitting was started with the simplest (a first order low-pass filter) and proceeded towards the more complex ones. The fitting was performed using the Levenberg-Marquardt -algorithm with a commercial computer program, Fig. P (Biosoft Ltd., Cambridge, UK). The fitted functions were ranked according to the quality of the fit as judged by the sum of squared error (SSE), and also by eye. The latter method is absolutely needed, because sometimes the fitting program may find—in multiparameter fitting—a local minimum of SSE that is still far form the best attainable fit. For obvious reasons, the fitted function was supposed to be the same for all frequency response, regardless of the size of the contrast stimulus or of the level of light adaptation.

The best fit was found to be a one containing no zeroes, one double pole and two second-order terms

$$\frac{K}{(1 + i\tau_1\omega)^2(1 + 2i\xi_2\tau_2\omega + (i\tau_2\omega)^2)(1 + 2i\xi_3\tau_3\omega + (i\tau_3\omega)^2)} \tag{8}$$

where K is a constant (defining asymptotic gain at low frequencies), ω is the natural frequency (i.e., $2\pi f$), the τ:s are the time constants and the ξ:s the damping factors of the system's elements. The second-order terms can be separated into first-order terms (the ξ:s are greater than one), when the photoreceptors are adapted to relatively low light levels (below 5,000 effective photons/s), but represent real resonances with higher adapting light levels. The result is very close to the one obtained by French (1980*a*,*b*) although he only used one adaptation level. Introduction of one or several nulls twisted the fit to be incompatible with the results. Addition of terms in the denominator did not increase the quality of the fit. The parameters yielded by the fitting procedure are given in Table I for all eight light backgrounds.

Calculation of Dead Time

The definition of dead time, or so-called pure time delay, includes that it does not affect the gain part of the frequency response. Instead it causes a phase lag that is proportional to the frequency of the stimulus and the length of the pure delay

$$\text{Phase}(f) = -2\pi f \Delta t \tag{9}$$

The dead time can be separated from the phase lag caused by the low-pass filtering itself (manifesting in the lowering gain in high frequencies). This was done by estimating the minimum phase gain (i.e., the gain of a system without any dead time)

TABLE I

The Parameters Obtained by Fitting the Gain Parts of the Frequency Response Functions

Background	τ_1	τ_2	τ_3	ξ_2	ξ_3
ph/s					
160	1.03	1.43	1.13	1.006	1.000
500	1.45	0.92	1.00	1.095	1.007
1,600	0.52	1.00	1.00	1.005	1.000
5,000	0.44	1.35	0.64	0.783	0.523
16,000	0.40	1.25	0.55	0.761	0.394
50,000	0.35	1.00	0.55	0.858	0.444
160,000	0.29	0.76	0.59	1.037	0.500
500,000	0.14	0.75	0.65	1.170	0.510

These parameters were used to calculate the phase corresponding to the gain parts, and subsequently for calculation of the dead time. The taus (τ_i) are given in milliseconds.

by an analytical function (see above), and subsequently calculating the corresponding phase function. This calculated phase was then subtracted from the phase that was determined experimentally, and the result was—by definition—the dead time. If this is true, then the calculated lag should be a linear function of frequency, as was found to be the case (Fig. 11 *B*).

We thank A. S. French, R. C. Hardie, J. Leppäluoto, and D. G. Stavenga for their interest and critical and constructive comments to this work.

This work has been supported by Orbis Sensorius in University of Oulu, Finland. M. Juusola was also funded by Finnish Medical Society Duodecim, Farmos Medical Research Co. and the Academy of Finland.

Original version received 3 August 1993 and accepted version received 2 May 1994.

REFERENCES

Bendat, J. S., and A. G. Piersol. 1971. Random Data: Analysis and Measurement Procedures. John Wiley and Sons, Inc., New York, London, Sydney, Toronto.

Borst, A. 1990. How do flies land? From behaviour to neuronal circuits. *BioScience.* 40:292–299.

Brown, J. E., L. J. Rubin, A. J. Ghalayini, A. P. Tarver, R. F. Irvine, M. J. Berridge, and R. E. Anderson. 1984. Myo-inositol polyphosphate may be a messenger for visual excitation in *Limulus* photoreceptors. *Nature.* 311:160–163.

Dodge, F. A., B. W. Knight, and J. Toyota. 1968. Voltage noise in *Limulus* visual cells. *Science.* 160:88–90.

Dubs, A. 1981. Non-linearity and light adaptation in the fly photoreceptor. *Journal of Comparative Physiology A.* 144:53–59.

Fein, A., R. Payne, D. W. Corson, M. J. Berridge, and R. F. Irvine. 1984. Photoreceptor excitation and adaptation by inositoll,4,5-trisphosphate. *Nature.* 311:157–160.

Fein, A., and R. Payne. 1989. Phototransduction in *Limulus* ventral photoreceptors: roles of calcium and inositol trisphosphate. *In* Facets of Vision. D. G. Stavenga and R. C. Hardie, editors. Springer Verlag, 173–185.

Franceschini, N., R. Chagneux, K. Kirschfeld, and A. Mücke. 1991. Vergence eye movements in flies. *In* Synapse-Transmission-Modulation. Proceedings of the 19th Göttingen Neurobiology Conference. N. Elsner and H. Penzlin, editors. Springer Verlag, Berlin. 275 pp.

French, A. S. 1980*a*. Coherence improvement in white noise analysis by the use of a repeated random sequence generator. *I.E.E.E. Transactions of Biomedical Engineering.* 27:51–53.

French, A. S. 1980*b*. Phototransduction in the fly compound eye exhibits temporal resonances and a pure time delay. *Nature.* 283:200–202.

French, A. S. 1980*c*. The linear dynamic properties of phototransduction in the fly compound eye. *Journal of Physiology.* 308:385–401.

French, A. S., and E. G. Butz. 1973. Measuring the Wiener kernels of a nonlinear system using the fast Fourier transform algorithm. *International Journal of Control.* 17:529–539.

French, A. S., A. V. Holden, and R. B. Stein. 1972. The estimation of the frequency response function of a mechanoreceptor. *Kybernetik.* 11:15–23.

French, A. S., M. Korenberg, M. Järvilehto, E. Kouvalainen, M. Juusola, and M. Weckström. 1993. The dynamic nonlinear behaviour of fly photoreceptors evoked by a wide range of light intensities. *Biophysical Journal.* In press.

Fuortes, M. G. F., and A. L. Hodgkin. 1964. Changes in time scale and sensitivity in the ommatidia of *Limulus*. *Journal of Physiology.* 172:239–263.

Fuortes, M. G. F., and S. Yeandle. 1964. Probability of occurrence of discrete potential waves in the eye of *Limulus*. *Journal of General Physiology.* 47:443–463.

Hardie, R. C. 1979. Electrophysiological analysis of the fly retina. I. Comparative properties of R1-6 and R7 and 8. *Journal of Comparative Physiology A.* 129:19–33.

Hardie, R. C. 1991. Whole cell recordings of the light induced current in dissociated *Drosophila* photoreceptors: evidence for feedback by calcium permeating the light-sensitive channels. *Proceedings of the Royal Society London B.* 245:203–210.

Hardie, R. C., and B. Minke. 1992. The *trp* gene is essential for a light-activated Ca^{2+} channel in *Drosophila* photoreceptors. *Neuron.* 8:643–651.

Harris, F. J. 1978. On the use of the windows for harmonic analysis with the discrete Fourier transform. *Proceedings of the IEEE.* 66:51–84.

Hengstenberg, R. 1971. Das Augenmuskelsystem der Stubenfliege *Musca domestica*. I. Analyse der "Clock-Spikes" und ihrer Quellen. *Kybernetik.* 9:56–77.

Hille, B. 1992. Ionic Channels of Excitable Membranes. Sinauer Associates, Inc., Sunderland, MA 607 pp.

Howard, J., B. Blakeslee, and S. B. Laughlin. 1987. The intracellular pupil mechanism and photoreceptor signal to noise ratios in the blowfly *Lucilia cuprina*. *Proceedings of the Royal Society London B.* 231:415–435.

Howard, J., A. Dubs, and R. Payne. 1984. The dynamics of phototransduction in insects: a comparative study. *Journal of Comparative Physiology A.* 154:707–718.

Howard, J., and A. W. Snyder. 1983. Transduction as limitation on compound eye function and design. *Proceedings of the Royal Society London B.* 217:287–307.

Johnson, D. E. 1976. Introduction to filter theory. Prentice-Hall, Englewood Cliffs, NJ. 307 pp.

Juusola, M. 1993. Linear and nonlinear contrast coding in light adapted blowfly photoreceptors. *Journal of Comparative Physiology A.* 172:511–521.

Juusola, M., and M. Weckström. 1993. Band-pass filtering by voltage-dependent membrane in an insect photoreceptor. *Neuroscience Letters.* 154:84–88.

Järvilehto, M., and F. Zettler. 1971. Localized intracellular potentials from pre- and postsynaptic components in the external plexiform layer of an insect retina. *Zeitschrift für der Vergleichende Physiologie.* 75:422–440.

Kouvalainen, E., M. Weckström, and M. Juusola. 1994. Determining the photoreceptor signal-to-noise ratio in the time and frequency domains with a pseudorandom stimulus *Visual Neuroscience.* In press.

Laughlin, S. B. 1981. A simple coding procedure enhances a neurone's information capacity. *Zeitschrift für Naturforschung.* 36c:910–912.

Laughlin, S. B. 1989. The role of sensory adaptation in retina. *Journal of Experimental Biology.* 146:39–62.

Laughlin, S. B., and R. C. Hardie. 1978. Common strategies for light adaptation in the peripheral visual systems of fly and dragonfly. *Journal of Comparative Physiology A.* 128:319–340.

Laughlin, S. B., and M. Weckström. 1989. The activation of a slow voltage-dependent potassium conductance is crucial for light adaptation in blowfly photoreceptors. *Journal of Physiology.* 418:200P.

Laughlin, S. B., and M. Weckström. 1993. Fast and slow photoreceptors: a comparative study of the functional diversity of coding and conductances in the Diptera. *Journal of Comparative Physiology A.* 172:593–609.

Lechleiter, J. D., and D. E. Clapham. 1992. Spiral waves and intracellular calcium signalling. *Journal de Physiologie.* 86:123–128.

Leutscher-Hazelhoff, J. T. 1975. Linear and non-linear performance of transducer and pupil in *Calliphora* retinula cells. *Journal of Physiology* 246:333–350.

Lillywhite, P. G. 1977. Single photon signals and transduction in an insect eye. *Journal of Comparative Physiology A.* 122:189–200.

Lillywhite, P. G., and S. B. Laughlin. 1979. Transducer noise in a photoreceptor. *Nature.* 227:569–572.

Marmarelis, P. Z., and V. Z. Marmarelis. 1978. Analysis of Physiological Systems: The White Noise Approach. Plenum Publishing Corp., NY. 487 pp.

Minke, B., and Z. Selinger. 1992. Inositol lipid pathway in fly photoreceptors: excitation calcium mobilisation and retinal degeneration. *In* Progress in Retinal Research. N. N. Osborne and G. L. Chader, editors. Pergamon Press, Oxford. 99–124.

Nagy, K. 1991. Biophysical processes in invertebrate photoreceptors: recent progress and a critical overview based on *Limulus* photoreceptors. *Quarterly Review of Biophysics.* 24:165–226.

Payne, R., D. W. Corson, A. Fein, and M. J. Berridge. 1986. Excitation and adaptation of *Limulus* ventral nerve photoreceptors by inositol 1,4,5 trisphosphate result from a rise in intracellular calcium. *Journal of General Physiology.* 88:127–142.

Payne, R., M. F. Flores, and A. Fein. 1990. Feedback inhibition by calcium limits the release of calcium by inositol trisphosphate in *Limulus* ventral photoreceptors. *Neuron.* 4:547–555.

Payne, R., B. Walz, S. Levy, and A. Fein. 1988. The localization of calcium release by inositol trisphosphate in *Limulus* photoreceptors and its control by negative feed-back. *Philosophical Transactions of the Royal Society London B.* 320:359–379.

Pinter, R. B. 1966. Sinusoidal and delta function responses of visual cells of the *Limulus* eye. *Journal of General Physiology.* 49:565–594.

Pinter, R. B. 1972. Frequency and time domain properties of retinular cells of the desert locust (*Schistocerca gregaria*) and the house crivket (*Acheta domesticus*). *Journal of Comparative Physiology.* 77:383–397.

Ranganathan, R., G. L. Harris, G. F. Stevens, and C. S. Zucker. 1991. A *Drosophila* mutant defective in extracellular calcium-dependent photoreceptor deactivation and rapid desensitization. *Nature.* 345:230–232.

Roebroek, J. G. H., and D. G. Stavenga. 1990. Insect pupil mechanism. IV. Spectral characteristics and light intensity dependence in the blowfly, *Calliphora erythrocephala*. *Journal of Comparative Physiology A*. 166:537–543.

Roebroek, J. G. H., M. van Tjonger, and D. G. Stavenga. 1990. Temperature dependence of receptor potential and noise in fly (*Calliphora erythocephala*) photoreceptor cells. *Journal of Insect Physiology*. 36:499–505.

Shapley, R. J. and C. Enroth-Cugell. 1984. Visual adaptation and retinal gain controls. *Progress in Retinal Research*. 3:263–346.

Smola, U. 1976. Voltage noise in insect visual cells. *In* Neural Principles in Vision. F. Zetter and R. Weiler, editors. Springer Verlag, New York. 194–213.

Spekreijse, H., and H. Oostings. 1970. Linearizing: a method for analysing and synthesizing non-linear systems. *Kybernetik*. 7:22–30.

Spekreijse, H., and L. H. van der Tweel. 1965. Linearization of evoked responses to sine wave-modulated light by noise. *Nature*. 205:913.

Srinivasan, M. V., and G. D. Bernard. 1975. The effect of motion on visual acuity of the compound eye: a theoretical analysis. *Vision Research*. 15:515–525.

Stavenga, D. G. 1989. Pigments in compound eyes. *In* Facets of Vision. D. G. Stavenga and R. C. Hardie, editors. Springer Verlag, NY. 152–172.

Stieve, H., J. Schnakenberg, A. Huhn, and H. Reuss. 1986. An automatic gain control in the *Limulus* photoreceptor. *In* Progress in Zoology. Membrane Control of Cellular Activity. Vol 33. H. C. Luttgau, editor. Gustav Fisher, Stuttgart. 367–376.

Suss-Toby, E., Z. Selinger, and B. Minke. 1991. Lanthanum reduces the excitation efficiency in fly photoreceptors. *Journal of General Physiology*. 89:849–868.

Weckström, M., R. C. Hardie, and S. B. Laughlin. 1991. Voltage-activated potassium channels in blowfly photoreceptors and their role in light adaptation. *Journal of Physiology*. 440:635–657.

Weckström, M., M. Juusola, and S. B. Laughlin. 1992. Presynaptic enhancement of signal transients in photoreceptor terminals in the compound eye. *Proceedings of the Royal Society London B*. 250:83–89.

Weckström, M., E. Kouvalainen, and M. Järvilehto. 1988. Non-linearities in response properties of insect visual cells: an analysis in time and frequency domain. *Acta Physiologica Scandinavia*. 132:103–113.

Wong, F. 1978. Nature of light-induced conductance changes in ventral photoreceptors of *Limulus*. *Nature*. 276:76–79.

Wong, F., B. W. Knight, and F. A. Dodge. 1982. Adapting bump model for ventral photoreceptors of *Limulus*. *Journal of General Physiology*. 79:1089–1113.

Wu, C-F., and W. L. Pak. 1978. Light-induced voltage noise in the photoreceptor of *Drosophila melanogaster*. *Journal of General Physiology*. 71:249–268.

Yeandle, S. 1958. Evidence for quantized slow potentials in the eye of *Limulus*. *American Journal of Ophthalmology*. 46:82–87.

Zettler, F. 1969. Die Abhängigkeit des Ubertragungsverhaltens von Frequenz und Adaptationszustand; gemessen am einzelnen Lichtrezeptor von *Calliphora erythocephala*. *Zeitschrift der Verglagende Physiologie*. 64:432–449.